HHS Public Access

Author manuscript

Mol Cancer Res. Author manuscript; available in PMC 2020 June 01.

Published in final edited form as:

Mol Cancer Res. 2019 June ; 17(6): 1294–1304. doi:10.1158/1541-7786.MCR-18-0963.

MCL1 and DEDD promote urothelial carcinoma progression

Andrew L. Hong[1,2,3], **Jennifer L. Guerriero**[2], **Mihir B. Doshi**[3], **Bryan D. Kynnap**[2], **Won Jun Kim**[2], **Anna C. Schinzel**[2], **Rebecca Modiste**[2], **Amy J. Schlauch**[2], **Rosalyn M. Adam**[1], **David J. Kwiatkowski**[2,4], **Rameen Beroukhim**[2,3], **Anthony Letai**[2], **Jonathan E. Rosenberg**[5,6,7], and **William C. Hahn**[2,3,4,7]

[1]Boston Children's Hospital, 300 Longwood Avenue, Boston, Massachusetts, 02115, USA

[2]Dana-Farber Cancer Institute, 450 Brookline Avenue, Boston, Massachusetts, 02215 USA

[3]Broad Institute of Harvard and MIT, 415 Main Street, Cambridge, Massachusetts, 02142 USA

[4]Brigham and Women's Hospital, 75 Francis Street, Boston, Massachusetts, 02115 USA

[5]Memorial Sloan Kettering Cancer Center, 1275 York Avenue, New York, New York 10065, USA.

[6]Weill Cornell Medical College, 1300 York Avenue, New York, NY 10065, USA.

[7]These authors jointly directed this work.

Abstract

Focal amplification of chromosome 1q23.3 in patients with advanced primary or relapsed urothelial carcinomas (UC) is associated with poor survival. We interrogated chromosome 1q23.3 and the nearby focal amplicon 1q21.3, as both are associated with increased lymph node disease in UC patients. Specifically, we assessed whether the oncogene *MCL1* that resides in 1q21.3 and the genes that reside in the 1q23.3 amplicon were required for the proliferation or survival of UC. We observed that suppressing MCL1 or the Death effector domain-containing protein (DEDD) in cells that harbor amplifications of 1q21.3 or 1q23.3, respectively, inhibited cell proliferation. We also found that overexpression of MCL1 or DEDD increased anchorage independence growth *in vitro* and increased experimental metastasis *in vivo* in the non-amplified UC cell line, RT112. Expression of MCL1 confers resistance to a range of apoptosis inducers while expression of

Corresponding author: William C. Hahn, M.D., Ph.D., Department of Medical Oncology, Dana-Farber Cancer Institute, 450 Brookline Avenue, Dana 1538, Boston, MA 02215, 617-632-2641 (phone), william_hahn@dfci.harvard.edu.

Author Information

Correspondence and requests for materials should be addressed to William C. Hahn (William_Hahn@dfci.harvard.edu).

Author Contributions

ALH, JER, WCH designed the study. ALH, JER and WCH wrote the manuscript. ACS developed the shRNA arrayed screen. ALH and AS performed the shRNA arrayed screens. JG developed and performed the BH3 profiling assays. ALH, BDK and MBD performed validation studies. RM performed the tail vein mouse experiments. ALH and ACS performed computational analyses. ALH, RA, DK, AL, JER, WCH supervised the studies. All authors discussed the results and implications and edited the manuscript.

The authors declare the following competing financial interests: J.L.G. receives sponsored research support from Eli Lilly and GlaxoSmithKline and is a paid consultant for GlaxoSmithKline. D.J.K. is a consultant for Genentech, AADi, and Novartis. R.B. receives sponsored research support from Novartis. A.L. is a consultant for AbbVie, receives sponsored research support from Novartis, AbbVie, Astra-Zeneca and is co-founder of Flash Therapeutics and Vivid Bioscience. J.E.R is a consultant for Lilly, Merck, Astellas, Seattle Genetics, Roche/Genentech, AstraZeneca/Medimmune, BMS, EMD Serono, Bayer, Inovio Pharmaceuticals, BioClin Therapeutics, QED Therapeutics, Adicet Bio, Sensei Biotherapeutics, Fortress Biotech, Pharmacyclics; has received honoraria from BMS, AstraZeneca, Chugai Pharma. W.C.H. is a consultant for Thermo Fisher, Paraxel, AjuIB, MPM Capital and is a founder and a member of the SAB for KSQ Therapeutics.

DEDD led to resistance to TNFα-induced apoptosis. These observations identify MCL1 and DEDD as genes that contribute to aggressive UC.

Introduction

In 2018, an estimated 81,190 patients will be diagnosed with urothelial carcinomas [UC, (1)]. 20–30% of these patients have muscle-invasive disease. UC patients that present with regional (7%) or distant (4%) disease have 5-year survival rates of 34.9% and 4.8% respectively (1). These survival rates, based on the use of platinum-based chemotherapies, have not changed for the past 20 years (2,3). Although advances in immunotherapy (e.g. pembrolizumab) have increased survival rates by three months in the relapsed setting, less than one-third of patients respond (4,5), and new therapies are clearly needed.

Several studies have enumerated that amplified genomic regions on chromosome 1q are associated with advanced UC (6–14). Muscle-invasive UC tumors harbor high level copy number gain of the 1q22–24 region (6,7). We and others showed through array comparative genomic hybridization (aCGH), molecular inversion probe (MIP) array technology, and multiplex ligation-dependent probe amplification (MLPA) that amplification of 1q23.3 is associated with poor survival and is more prevalent in metastatic samples (11,13,14). Several genes including *PRRC2C* (9), *BCL9, CHD1L, MCL1, SETDB1, HIF1B*, and *PFDN2* (10,12) have been shown to be recurrently amplified in UC tumors.

Recently, the Cancer Genome Atlas (TCGA) sequenced UC tumors from 412 patients and we confirmed that 1q23.3 is focally amplified in UC and associated with higher disease stage. In addition, 1q21.3 was also found to be recurrently amplified (15). Here we interrogated genes resident in 1q21.3 and 1q23.3 to identify genes involved in the survival or progression of UC.

Materials and Methods:

Cell lines:

Cell lines SCABER, HT1376, JMSU, RT112, RT4, HT1197, SW780 and T24 were obtained from the Biological Samples Platform at the Broad Institute of Harvard and MIT in 2012. UM-UC10 was provided by the Kwiatokowski lab in 2012. TRT-HU1 was provided by the Adam lab in 2013. Cells were screened for mycoplasma by PCR testing. Cell lines used for secondary validation studies (e.g. HT1376, JMSU, RT4, RT112 and TRT-HU1) were confirmed by Fluidigm SNP fingerprinting over the course of the experiments. Cells were kept in culture a maximum of 2 months prior to thawing of a new aliquot to limit genetic drift.

shRNA arrayed screen:

Lentivirus of individual shRNAs was produced at the Broad Institute and arrayed in two 96 well plates. Each cell line was optimized for viral toxicity, polybrene sensitivity, puromycin sensitivity and proliferation rates. Cells were seeded on day -1 in a 384 well plate. Lentivirus was introduced on day 0 and cells were spin-infected for 30 minutes. Equal amounts of

media with puromycin selection were added on day 1 and cells were monitored over the course of 7 days. At day 7, cells were treated with Cell-TiterGlo (Promega) and levels were read on an Envision plate reader (Perkin Elmer).

Open Reading Frame vectors:

ORFs for DEDD, F11R, MCL1, PVRL4 were obtained from the Human ORFeome 8.1 collection at Dana-Farber Cancer Institute. ARHGAP30 was synthesized by Genscript and sequence verified (Piscataway Township, NJ). We confirmed overexpression of these genes by immunoblot using a V5 antibody.

Anchorage independence by soft agar:

In a 6 well plate, agar was prepared with media such that the bottom layer was 0.6% agar and top layer was 0.3% agar. Cells were grown in log phase, counted on a ViCell (Beckman Coulter, Brea, CA) and mixed into the top layer. Cells were monitored over 2–4 weeks depending on the cell line. Images were captured on an Olympus SZX9 inverted microscope and analyzed using ImageJ (NIH, Bethesda, MD). Experiments were performed in biological triplicates.

Proliferation studies:

After confirmation that cells overexpressed the gene of interest, cells were seeded in technical triplicates in 6 well plates. Plates were read at the specified times and counted on a ViCell. Experiments were performed in biological duplicates for TRT-HU1 and biological triplicates for RT4 and RT112.

BH3 profiling:

Cells and supernatant were harvested at log phase and plated into a 384 well plate in the respective growth media. Cells were then treated with the BH3 mimetic and concentration as noted in the figure. Cells were then assessed for MOMP activity as previously published (16). Experiments were performed in biological triplicates.

Compound treatments:

Cells were treated with TRAIL, TNFα (R&D Systems, Minneapolis, MN), cycloheximide (Cell Signaling Technologies, Danvers, MA), MK2206 for the specified times as noted in the figure legends. These were then assayed either by CellTiterGlo, CaspaseGlo 3/7 and 8 (Promega, Madison, WI) per established protocols. Experiments were performed with technical triplicates and were repeated a minimum of two times for biological replicates.

Immunoblots:

Cells were lysed with RIPA buffer (Cell Signaling Technologies, Danvers, MA) containing protease inhibitors (cOmplete, Roche) and phosphatase inhibitors (PhosSTOP, Roche). Antibodies used were as follows: TNF-R1 (H-5; sc-8436; 1:500), NFkB p50 (H-119; sc-7178; 1:500), beta-actin (C4; sc-47778; 1: 10,000) from Santa Cruz Biotechnology, V5/HRP (R961–25; 1: 2,000) from Invitrogen, Pan-Akt (2920: 1: 1,000), Phospho-Akt (4060; 1: 1,000), FADD (2782; 1: 1,000) from Cell Signaling Technologies.

In vivo tumor injections and experimental metastases:

This research project has been approved under an IRB approved protocol at Dana-Farber Cancer Institute. This research project has been reviewed by the Institutional Animal Care and Use Committee (IACUC) and is in compliance with the Animal Welfare Act and the Office of Laboratory Welfare (OLAW) of the National Institutes of Health (NIH). The FUW-Luc-mCherry-puro vector was introduced into parental RT112 cells (17). Once stable lines were generated, we then introduced the ORFs into these cells and selected the cells with puromycin and blasticidin. Cells were confirmed to have mCherry expression as a surrogate the vector was introduced properly by flow cytometry using the BD J-Fortessa (Billerica, MA). Cells were subsequently grown in log phase and injected in to the tail vein of mice. Female CrTac:NCr-*Foxn1*^{nu} mice ages 6–8 weeks were used in this study (Taconic Laboratories, Rensselaer, NY). In one experiment, we used 250,000 cells (n=3 mice per ORF) and in the other we used 500,000 cells (n=5 mice per ORF). Mice were monitored for weight and health over the course of the experiment with BLI imaging performed at every 2-week timepoints.

Immunohistochemistry:

All IHC was performed on the Leica Bond automated staining platform using the Leica Biosystems Refine Detection Kit with citrate antigen retrieval. Antibodies used include: Ki-67(CRM325 clone D20B12; 1:400) from Biocare and Cleaved Caspase-3 from CST (9664 clone Asp175/5A1E; 1:250).

Accession codes:

Not applicable.

Data Availability:

All primary data are available from the authors. Noted plasmids in the text are available through Addgene or the Genomics Perturbations Platform at the Broad Institute of Harvard and MIT.

Results

1q21.3 and 1q23.3 are associated with higher disease stage in UC

Analysis of Affymetrix SNP6.0 segmented copy-number TCGA data from patients with UC identified 37 recurrent focal amplifications and 36 recurrent focal deletions (q-values <0.25) based on Genomic Identification of Significant Targets in Cancer (GISTIC) 2.0 analyses (18,19). We focused our efforts on the amplifications to identify recurrent amplified genes that are required for the proliferation or survival of patients with advanced UC. 6p22.3 was the most significantly focal amplicon in UC with a q-value 7.03e-82 and harbors *SOX4*, a master regulator of epithelial-mesenchymal transition (EMT) (Figure 1a) (20). The second most significant focal amplification was 1q23.3 with a q-value of 6.28e-56 (Figure 1a). The 1q23.3 amplicon has a wider GISTIC amplification peak suggesting that a nearby focal amplicon may be a confounding factor. Indeed, 1q21.3 is the 6th most significant focal amplicon with a q-value of 3.52e-28 (Figure 1a–b).

We then assessed whether any of the 13 clinical features assessed in TCGA correlated with these 37 focal amplifications (21). We found that copy number gain of 1q21.3 was correlated with increased pathologic nodal staging (q-value = 0.223 and p-value = 0.00575; Figure 1c). In addition, copy number gain of 1q23.3 was correlated with age (e.g. older patients were likely to have amplification of 1q23.3; q-value = 0.228) and increased pathologic nodal staging (q-value of 0.171, p value = 0.00255; Figure 1d). Patients with a diagnosis of UC and with increased nodal staging are at higher risk of recurrence and have overall poorer survival (22). Therefore, we concluded that focal amplification of 1q21.3 or 1q23.3 is likely associated with and may be a driver of poor outcome in UC.

The 1q21.3 amplicon encompasses 13 genes (Table 1) including *MCL1*, an oncogene that was previously identified in a study of 3,131 copy-number profiles across a number of cancers (23). *MCL1* has been shown to be critical for regulation of apoptosis in lymphocyte development (24) and found to be overexpressed or amplified in follicular lymphoma, diffuse large B-cell lymphoma, and lung and breast cancers but its role in UC is unknown (23,25). *MCL1* has also been found to be amplified in 11% of cases in a cohort of 35 patients with stage IV UCs (26). Analysis of the UC TCGA data identified 11.8% of patients (n=48 of 408 patients) with amplification of *MCL1* (Table S1) (15).

We previously studied three advanced UC cohorts and identified a 1q23.3 focal amplicon that was associated with poor survival (13). Within this amplicon we found 5 genes that were associated with poor survival: *F11R, PFDN2, DEDD, USP21* and *PPOX*. The TCGA studies identified a similar 1q23.3 focal amplicon that included 7 genes (2 that overlapped with our studies): *F11R, TSTD1, USF1, AG30, PVRL4, KLHDC9*, and *PFDN2*. These 10 genes spanned chromosome 1 at 160,965,001 bp - 161,171,218 bp. When we examined this region for any additional genes that were not found in either study, we identified *NIT1* and *UFC1*. We assessed these 12 genes in this study (Table 2). Of these genes, *PFDN2* has previously been identified as amplified in UC urine DNA (12). In addition, *PVRL4* has been identified to have tumorigenic potential in breast cancer (27). Compared to the 1q21.3 amplicon where *MCL1* is the likely gene that leads to tumorigenesis in UC, the 1q23.3 amplicon remains less well studied. Furthermore, analysis of the UC TCGA showed that expression of these genes correlated with amplification status (Pearson correlation range 0.2470 to 0.8794 with associated q-values between 0 to 0.003; Figure 1e and Table S2). Here we focused our efforts on determining the function of MCL1 overexpression in UC and performed a systematic analysis of the 12 genes identified in the 1q23.3 amplicon.

UC cell lines that harbor 1q amplifications depend on MCL1 in 1q21.3 and DEDD or ARHGAP30 in 1q23.3

To validate *MCL1* and identify genes required for the proliferation/survival of UC cells that harbor 1q23.3 amplicon, we used RNAi to determine whether *MCL1* or genes resident in the 1q23.3 focal amplicon were required for survival (Figure 2a). We first identified a set of urothelial carcinoma cell lines which harbored gains or amplifications of 1q23.3 and/or *MCL1* based on Affymetrix SNP6.0 arrays or our prior work (Table S3) (11,28). Of cell lines with gains or amplifications of 1q23.3 and/or *MCL1*, we chose four cell lines, SCABER, UM-UC10, HT-1376 and JMSU for further analyses. We also included 5 lines

that lacked gain or amplification of *MCL1* and/or 1q23.3: RT-4, RT-112, HT-1197, SW-780 and T24.

We then designed an arrayed shRNA screen of 81 shRNAs: 71 shRNAs targeting 13 genes (*MCL1* in 1q21.3 and 12 genes identified in 1q23.3) and 10 controls (e.g. empty, RFP, Luciferase, GFP) (Table S4). After introducing shRNAs targeting these genes into cells that do or do not harbor amplifications of 1q21.3 or 1q23.3, we measured proliferation/viability by CellTiter Glo. We confirmed that the expression of the control shRNAs did not lead to significant viability changes in the cell lines (Figure 2b). We then compared the viability of the cells following RNAi between UC cell lines with amplification of 1q23.3 to the non-amplified cell lines (Figure 2c and 2d). Individual shRNAs were then collapsed to consensus gene dependencies using RNAi Gene Enrichment Ranking (RIGER) (29). *MCL1* in 1q21.3 and *ARHGAP30* and *DEDD* in 1q23.3 scored as essential for the proliferation/survival of 1q amplified cell lines with a p-value <0.05 (Table S5).

MCL1, ARHGAP30 or DEDD is necessary but not sufficient to drive UC proliferation and anchorage independent growth

We then performed studies to determine whether overexpression of MCL1, ARHGAP30 or DEDD induced tumorigenic potential to urothelial cell lines. We first assessed the effects of overexpression in a hTERT-immortalized urothelial cell line, TRT-HU1. We used overexpression of $HRAS^{G12V}$, a well characterized oncogene that is necessary for tumor formation in UC, as a positive control (30–32). We then overexpressed luciferase, ARHGAP30, DEDD or MCL1 in TRT-HU1 (Figure S1a-b). We calculated population doublings by assessing cell counts with trypan blue exclusion. In the TRT-HU1 immortalized bladder cell line, $HRAS^{G12V}$ cells doubled 1.50 times faster than luciferase overexpressing cells. ARHGAP30, DEDD or MCL1 overexpressed cells proliferated at a similar rate to that of luciferase overexpressing cells (0.86x – 0.99x; Figure S1c). Therefore, expressing ARHGAP30, DEDD or MCL1 in hTERT-immortalized cells did not affect cell proliferation.

We then overexpressed luciferase, ARHGAP30, DEDD or MCL1 in the UC cell lines, RT4 and RT112. In RT4, Luciferase overexpressing cells doubled 18.4 times during the time course of this experiment. ARHGAP30 cells proliferated at the same rate (1.04 times) as the luciferase cells while cells overexpressing MCL1 or DEDD doubled 1.33 or 1.40 times faster (Figure 2e). In the RT112 cell line, luciferase overexpressing cells doubled 24.6 times during the time course of the experiment. MCL1 doubled 1.24 times faster, ARHGAP30 doubled 1.28 times faster and DEDD doubled 1.20 times faster than luciferase (Figure 2f). In these UC cell lines, we found that cells overexpressing MCL1 and DEDD proliferated moderately more compared to cells overexpressing luciferase.

We then assessed whether expression of these genes conferred anchorage independent growth. We began with the non-UC TRT-HU1 cells to determine if overexpression of the gene of interest would lead to colonies in soft agar in an immortalized urothelial cell line. This cell line harbors a large deletion in the short arm chromosome 9p where *CDKNA2* resides but does not form anchorage independent colonies (30). Expression of $HRAS^{G12V}$ conferred anchorage independent growth (p-value 0.023; Figure S1d), but none of other

genes induced anchorage independent growth (Figure S1d). These findings indicated that expression of *MCL1* in 1q21.3 or *ARHGAP30* or *DEDD* in 1q23.3 failed to induce anchorage independent growth in an immortalized urothelial cell line.

We then assessed anchorage independent growth in the UC cell line, RT112. RT112 harbors a *FGFR3* amplification, forms subcutaneous tumors and does not harbor gain or amplification of *MCL1* or 1q23.3 (32). We asked whether overexpression of the 3 genes identified from the RNAi screen leads to anchorage independence in RT112. Overexpression of MCL1 (p-value 0.0001), ARHGAP30 (p-value 0.0054) and DEDD (p-value 0.0058) conferred a significant increase in colony formation compared to controls hcRed and Luciferase (Figure 2g). Specifically, DEDD overexpression led to an average 2.3-fold increase in colony formation while MCL1 expression induced a 4.4-fold increase and ARHGAP30 had a 3.8-fold increase compared to hcRed and Luciferase. These observations indicate that expression of these three genes conferred anchorage independent growth on the RT112 cells.

Taken together, we did not observe a proliferation advantage or anchorage independent growth of immortalized urothelial cells overexpressing MCL1, ARHGAP30 or DEDD. In UC cell lines, we saw overexpression of MCL1 or DEDD led to a modest proliferation advantage and anchorage independent growth.

MCL1 but not DEDD overexpression leads to resistance to intrinsic mitochondrial dependent apoptosis

Based on the loss- and gain- of function assays, we then focused our efforts on understanding mechanisms by which MCL1 (1q21.3) and DEDD (1q23.3) conferred a fitness advantage in UC. Prior work has established that MCL1 inhibits apoptosis while DEDD harbors a death-effector domain (DED) but its role in apoptosis remains unclear (33,34).

We first assessed the baseline apoptotic potential of these cells when MCL1 or DEDD were overexpressed by measuring caspase 3/7 levels. We found that overexpression of DEDD led to no significant difference to cells overexpressing LacZ (p-value 0.82) whereas overexpression of MCL1 led to a 24% decrease in caspase 3/7 levels (p-value 3.13e-7; Figure S2a).

We then began with assessing the intrinsic apoptotic pathway. We utilized the BH3 profiling assay, which assesses the mitochondrial outer membrane permeabilization (MOMP) induced by a exposure of mitochondria to a panel of synthetic BH3 peptides (35). We expressed LacZ, MCL1, or DEDD in TRT-HU1, RT4 and RT112 bladder cell lines. For each of the cell lines overexpressing LacZ, we established baseline levels of MOMP with various BH3 peptides (Figure 3). We then compared these profiles to cell lines overexpressing MCL1 or DEDD. When we overexpressed MCL1, we observed decreased MOMP induced by nearly all BH3 peptides across all three cell lines (Figure 3a–c). We performed similar BH3 profiling studies with DEDD overexpression across the TRT-HU1, RT4 and RT112 cell lines and found no significant changes in MOMP levels after exposure to all BH3 mimetics (Figure S2b–d).

These findings suggest that MCL1 is and DEDD is not involved in the intrinsic mitochondrial mediated apoptotic cascade.

MCL1 or DEDD overexpression leads to resistance to extrinsic-apoptosis

We then assessed two extrinsic apoptosis pathways using the RT112 cell line: TNF-related apoptosis-inducing ligand (TRAIL) and TNFα induced apoptosis. We first looked at cell viability as assessed by Cell-TiterGlo when LacZ, MCL1 or DEDD were overexpressed and treated with increasing doses of TRAIL. MCL1 has previously been shown to resist TRAIL-induced apoptosis in other cancer types (36). Overexpression of MCL1 lead to resistance to cell death upon TRAIL treatment in UC. However, we failed to observe resistance to TRAIL-induced apoptosis when DEDD was overexpressed (Figure 4a).

We then looked at the effects on cell proliferation upon TNFα treatment with Cell-TiterGlo. Overexpression of DEDD led to similar resistance to TNFα treatment as MCL1 when compared to Luciferase (Figure 4b). Specifically, upon treatment with TNFα, 63.7% of cells remained alive as compared to a no treatment control. 81.2% of cells remained alive when MCL1 was overexpressed (p-value 0.024) and 79.2% of cells remained alive when DEDD was overexpressed (p-value 0.037) suggesting both genes when overexpressed lead to resistance to TNFα-induced cell death. We then assessed the extrinsic apoptotic pathway by measuring caspase 8 activity and downstream caspase 3/7 activity when cells overexpressing LacZ, MCL1 or DEDD were treated with TNFα. Compared to the LacZ control, we found that there was a consistent decrease of Caspase 8 activation of 54.2% with MCL1 overexpression and a decrease of 26.9% with DEDD overexpression (Figure 4c). We saw a similar response for activation of Caspase 3/7 (Figure 4d). We further assessed proteins upstream of caspase 8, TNFR1 and NFkB p105/p50 by immunoblotting and failed to observe any differences between cells expressing LacZ and DEDD or MCL1 (Figure S3a).

TNFα mediated apoptosis via caspase 8 can be potentiated by a protein synthesis inhibitor such as cycloheximide (37). Cycloheximide (CHX) treatment eliminates c-FLIP, an endogenous caspase-8 inhibitor (37). With LacZ overexpression, co-treatment with CHX potentiated a more pronounced decrease in cell viability as measured by Cell-TiterGlo compared to TNFα treatment alone (Figure 4b and e). DEDD overexpression led to a log fold increase in resistance to TNFα treatment (Figure 4e). MCL1 overexpressed cells remained resistant across the full dose range despite the addition of CHX treatment (Figure 4e).

Recent studies suggest that DEDD supports the stability of Akt in mouse models (38). We assessed Akt and phosphorylated Akt levels in the cells overexpressing LacZ, MCL1 or DEDD. We found a modest increase in baseline Akt levels but noted an increase in phosphorylated Akt, particularly following TNFα treatment (Figure 4f). We then treated these cells with a pan-Akt inhibitor, MK2206, at 100nM along with increasing doses of TNFα. Here, we saw that although there was no significant change to how cells overexpressing LacZ responded to TNFα and MK2206 (Figures 4e and g), cells overexpressing DEDD became similarly sensitive to TNFα treatment. This suggests that DEDD overexpression and function are in part dependent upon Akt function (Figure 4g).

Although overexpression of MCL1 or DEDD leads to resistance to extrinsic apoptosis, we failed to see resistance to platinum-based therapies (Fig S3b), which are the standard of care in patients with urothelial carcinomas. These findings suggest that in addition to resisting intrinsic and TRAIL-induced apoptosis, MCL1 overexpression induces resistance to TNFα-induced apoptosis. In contrast, DEDD overexpression only confers resistance to TNFα-induced apoptosis that is in driven in part by Akt and can be abrogated with the pan-Akt inhibitor, MK-2206.

Overexpression of MCL1 or DEDD induces metastases in vivo

Since gain of 1q21.3 or 1q23.3 is correlated with increased nodal staging (Figure 1b and c), we hypothesized that the genes implicated in these regions would lead to increased metastasis *in vivo*. We performed an experimental metastases assay to assess the ability of RT112 cells overexpressing MCL1 or DEDD to develop metastases following tail vein injection. To monitor the evolution and effects of these metastases, we introduced a luciferase expressing vector that would enable monitoring of tumor formation using bioluminescent imaging [BLI; Methods; (17)].

We then introduced LacZ (control), MCL1 and DEDD into these cells. Prior studies in NIH 3T3 cells have shown that Hras-transfected cells led to experimental metastasis (39,40). We introduced $HRAS^{G12V}$ into the RT112 luciferase expressing cells as the positive control. We then injected these cells via the tail vein in immunodeficient mice. We monitored the mice for lung metastasis and other metastatic sites based on BLI measurements. By day 56, we observed a significant difference between BLI measurements of MCL1, DEDD and $HRAS^{G12V}$ overexpressed cells compared to LacZ controls (Figure 5a–b) but no significant difference between $HRAS^{G12V}$ and MCL1 (p-value 0.154) or DEDD (p-value 0.093).

Furthermore, we found that mice harboring cells overexpressing MCL1, DEDD or $HRAS^{G12V}$ exhibited significant mortality as compared to mice injected with cells overexpressing LacZ (Figure 5c). Specifically, the median survival for cells overexpressing MCL1 was 103 days, DEDD 153.5 days and $HRAS^{G12V}$ 119.5 days, while mice expressing LacZ survived to the end of the experiment. The tumors formed at the time of sacrifice were consistent with a urothelial carcinoma, and there were no notable morphologic differences between the tumors overexpressing the various genes (Figure 5d). Finally, we assessed baseline apoptosis with cleaved caspase-3 and proliferation with Ki-67 on the lung tumors with overexpression of MCL1, DEDD and $HRAS^{G12V}$. We failed to find a significant difference between MCL1 or DEDD as compared to $HRAS^{G12V}$ showing that the modest proliferative advantage seen *in vitro* when MCL1 or DEDD is overexpressed (Figure 2f) is also seen *in vivo* (Figures S3c–d). These findings show overexpression of MCL1 or DEDD in RT112 cells leads to *in vivo* metastasis.

Discussion

Therapy for advanced urothelial carcinomas remains unchanged for several decades until recent advances with immunotherapy (4,41). Although these advances have increased survival by 3 months (from 7.4 months to 10.3 months) in the relapsed setting following platinum-based chemotherapy, additional therapy and biomarkers are needed to improve

survival. Our initial studies of focal amplicons in advanced UC identified the region of chromosome 1q23.3. Analysis of the larger cohort of patients in UC TCGA identified a nearby and potentially confounding focal amplicon on chromosome 1q21.3. We have interrogated both of these regions in this study. We took a targeted approach in 1q21.3 as *MCL1*, a putative oncogene was identified by GISTIC to be a potential target gene in this region for UC patients. We took a broader and systematic approach to the region of 1q23.3 and assessed the function of 12 genes in this region. We have validated *MCL1* as an oncogene in UC and identified *DEDD* as a potential oncogene. Both are necessary but not sufficient for tumor maintenance. Suppression of MCL1 or DEDD leads to viability/proliferation defects in UC cell lines that have gain or amplification of amplicons that harbor these genes. MCL1 or DEDD overexpression provided a modest proliferative advantage, increases anchorage independence by soft agar assay and has markedly enhanced the ability of UC cell lines to form lung metastases, similar to the effects of $HRAS^{G12V}$.

MCL1, a putative oncogene in various cancer lineages, has not been functionally tested within UC although MCL1 overexpression by RNA-seq is seen in 5% of patients in TCGA (n=412). We found that MCL1 overexpression leads to resistance to both intrinsic and extrinsic apoptotic pathways, similar to effects of MCL1 in other cancer lineages (42,43).

Studies in 293T cells overexpressing DEDD suggested that DEDD had both apoptotic and anti-apoptotic roles (33). Our findings suggest that DEDD overexpression in UC cell lines enhances total Akt and phospho-Akt levels and resists apoptosis (Figure 6). Although DEDD does not have a role in intrinsic apoptosis as compared to MCL1, we found that it has a role in the extrinsic pathway, specifically through resistance to TNFα mediated apoptosis. The resistance to TNFα mediated apoptosis is abrogated when a pan-Akt inhibitor was used (MK2206) which further supports a role for Akt in DEDD overexpression.

We have shown that individually, MCL1 and DEDD are able to confer tumorigenic properties. Furthermore, we have shown that overexpression of DEDD or MCL1 *in vivo* leads to increased metastatic potential as measured by tail-vein injection studies. These findings now identify both DEDD and MCL1 as therapeutic targets in urothelial carcinomas.

Supplementary Material

Refer to Web version on PubMed Central for supplementary material.

Acknowledgements

We thank the Hahn lab, Cichowski lab, Rosalind Segal, Charles W.M. Roberts and Kimberly Stegmaier for critical discussions and/or reading of the manuscript. We thank Paul Kirschmeier and the Lurie Family Imaging Center at Dana Farber Cancer Institute. The results published here are in part based upon data generated by the TCGA Research Network: http://cancergenome.nih.gov/. We thank Dana-Farber/Harvard Cancer Center in Boston, MA, for the use of the Rodent Histopathology Core and the Specialized Histopathology Core which provided histology, immunohistochemistry service, slide interpretation and histopathological interpretation. The human ORFeome collection is made possible through support from the High-Tech Fund of the Dana-Farber Cancer Institute, The Ellison Foundation (Boston, MA), and by grants from the National Cancer Institute, the National Human Genome Research Institute, and the National Institute of General Medical Sciences. This work was supported in part by the NCI U01 CA176058 (W. Hahn), NCI R21 CA164613 (J. Rosenberg, W. Hahn), AACR-Conquer Cancer Foundation of ASCO Young Investigator Translational Cancer Research Award 14–40-31-HONG (A. Hong), NIH T32 CA136432 (A. Hong), NIH K12 HD052896–08 (A. Hong), NCI P50 CA101942 (A. Hong), American Cancer Society MRSG-18–202-01-TBG (A. Hong) and NIH F32 CA180733 (J. Guerriero). This work was supported in

part by the NCI Cancer Center Support Grants NIH P30 CA06516 (Dana-Farber/Harvard Cancer Center) and NIH P30 CA008748 (Memorial Sloan Kettering Cancer Center).

References

1. Noone AM, Howlader N, Krapcho M, Miller D, Brest A, Yu M, et al. Cancer Statistics Review, 1975–2015 - SEER Statistics [Internet]. [cited 2018 May 6]. Available from: https://seer.cancer.gov/csr/1975_2015/
2. von der Maase H, Sengelov L, Roberts JT, Ricci S, Dogliotti L, Oliver T, et al. Long-term survival results of a randomized trial comparing gemcitabine plus cisplatin, with methotrexate, vinblastine, doxorubicin, plus cisplatin in patients with bladder cancer. Journal of clinical oncology: official journal of the American Society of Clinical Oncology. 2005;23:4602–8. [PubMed: 16034041]
3. Grossman HB, Natale RB, Tangen CM, Speights VO, Vogelzang NJ, Trump DL, et al. Neoadjuvant chemotherapy plus cystectomy compared with cystectomy alone for locally advanced bladder cancer. The New England journal of medicine. 2003;349:859–66. [PubMed: 12944571]
4. Bellmunt J, de Wit R, Vaughn DJ, Fradet Y, Lee JL, Fong L, et al. Pembrolizumab as Second-Line Therapy for Advanced Urothelial Carcinoma. The New England journal of medicine. 2017;376:1015–26. [PubMed: 28212060]
5. Dietrich B, Srinivas S. Urothelial carcinoma: the evolving landscape of immunotherapy for patients with advanced disease. Res Rep Urol. 2018;10:7–16. [PubMed: 29417045]
6. Richter J, Jiang F, Gorog JP, Sartorius G, Egenter C, Gasser TC, et al. Marked genetic differences between stage pTa and stage pT1 papillary bladder cancer detected by comparative genomic hybridization. Cancer research. 1997;57:2860–4. [PubMed: 9230190]
7. Simon R, Burger H, Brinkschmidt C, Bocker W, Hertle L, Terpe HJ. Chromosomal aberrations associated with invasion in papillary superficial bladder cancer. The Journal of pathology. 1998;185:345–51. [PubMed: 9828832]
8. Hoglund M, Sall T, Heim S, Mitelman F, Mandahl N, Fadl-Elmula I. Identification of cytogenetic subgroups and karyotypic pathways in transitional cell carcinoma. Cancer research. 2001;61:8241–6. [PubMed: 11719456]
9. Huang WC, Taylor S, Nguyen TB, Tomaszewski JE, Libertino JA, Malkowicz SB, et al. KIAA1096, a gene on chromosome 1q, is amplified and overexpressed in bladder cancer. DNA and cell biology. 2002;21:707–15. [PubMed: 12443540]
10. Eriksson P, Aine M, Sjodahl G, Staaf J, Lindgren D, Hoglund M. Detailed Analysis of Focal Chromosome Arm 1q and 6p Amplifications in Urothelial Carcinoma Reveals Complex Genomic Events on 1q, and SOX4 as a Possible Auxiliary Target on 6p. PloS one. 2013;8:e67222. [PubMed: 23825644]
11. Chekaluk Y, Wu CL, Rosenberg J, Riester M, Dai Q, Lin S, et al. Identification of nine genomic regions of amplification in urothelial carcinoma, correlation with stage, and potential prognostic and therapeutic value. PloS one. 2013;8:e60927. [PubMed: 23593348]
12. Lopez V, Gonzalez-Peramato P, Suela J, Serrano A, Algaba F, Cigudosa JC, et al. Identification of prefoldin amplification (1q23.3-q24.1) in bladder cancer using comparative genomic hybridization (CGH) arrays of urinary DNA. Journal of translational medicine. 2013;11:182. [PubMed: 23914742]
13. Riester M, Werner L, Bellmunt J, Selvarajah S, Guancial EA, Weir BA, et al. Integrative analysis of 1q23.3 copy number gain in metastatic urothelial carcinoma. Clinical cancer research: an official journal of the American Association for Cancer Research. 2014;
14. Bambury RM, Bhatt AS, Riester M, Pedamallu CS, Duke F, Bellmunt J, et al. DNA copy number analysis of metastatic urothelial carcinoma with comparison to primary tumors. BMC cancer. 2015;15:2. [PubMed: 26187043]
15. Robertson AG, Kim J, Al-Ahmadie H, Bellmunt J, Guo G, Cherniack AD, et al. Comprehensive Molecular Characterization of Muscle-Invasive Bladder Cancer. Cell. 2017;171:540–556.e25. [PubMed: 28988769]
16. Touzeau C, Ryan J, Guerriero J, Moreau P, Chonghaile TN, Le Gouill S, et al. BH3 profiling identifies heterogeneous dependency on Bcl-2 family members in multiple myeloma and predicts sensitivity to BH3 mimetics. Leukemia. 2016;30:761–4. [PubMed: 26174630]

17. Kimbrel EA, Davis TN, Bradner JE, Kung AL. In vivo pharmacodynamic imaging of proteasome inhibition. Molecular imaging. 2009;8:140–7. [PubMed: 19723471]
18. Broad Institute TCGA Genome Data Analysis Center. SNP6 Copy number analysis (GISTIC2). Broad Institute of MIT and Harvard; 2016.
19. Mermel CH, Schumacher SE, Hill B, Meyerson ML, Beroukhim R, Getz G. GISTIC2.0 facilitates sensitive and confident localization of the targets of focal somatic copy-number alteration in human cancers. Genome biology. 2011;12:r41 Epub 2011 Apr 28. [PubMed: 21527027]
20. Tiwari N, Tiwari VK, Waldmeier L, Balwierz PJ, Arnold P, Pachkov M, et al. Sox4 is a master regulator of epithelial-mesenchymal transition by controlling Ezh2 expression and epigenetic reprogramming. Cancer cell. 2013;23:768–83. [PubMed: 23764001]
21. Broad Institute TCGA Genome Data Analysis Center. Correlation between copy number variation genes (focal events) and selected clinical features. Broad Institute of MIT and Harvard; 2016.
22. Stein JP, Lieskovsky G, Cote R, Groshen S, Feng A-C, Boyd S, et al. Radical Cystectomy in the Treatment of Invasive Bladder Cancer: Long-Term Results in 1,054 Patients. JCO. 2001;19:666–75.
23. Beroukhim R, Mermel CH, Porter D, Wei G, Raychaudhuri S, Donovan J, et al. The landscape of somatic copy-number alteration across human cancers. Nature. 2010;463:899–905. [PubMed: 20164920]
24. Opferman JT, Letai A, Beard C, Sorcinelli MD, Ong CC, Korsmeyer SJ. Development and maintenance of B and T lymphocytes requires antiapoptotic MCL-1. Nature. 2003;426:671–6. [PubMed: 14668867]
25. Zhou P, Levy NB, Xie H, Qian L, Lee CY, Gascoyne RD, et al. MCL1 transgenic mice exhibit a high incidence of B-cell lymphoma manifested as a spectrum of histologic subtypes. Blood. 2001;97:3902–9. [PubMed: 11389033]
26. Ross JS, Wang K, Al-Rohil RN, Nazeer T, Sheehan CE, Otto GA, et al. Advanced urothelial carcinoma: next-generation sequencing reveals diverse genomic alterations and targets of therapy. Modern pathology: an official journal of the United States and Canadian Academy of Pathology, Inc 2013;
27. Pavlova NN, Pallasch C, Elia AE, Braun CJ, Westbrook TF, Hemann M, et al. A role for PVRL4-driven cell-cell interactions in tumorigenesis. eLife. 2013;2:e00358. [PubMed: 23682311]
28. Barretina J, Caponigro G, Stransky N, Venkatesan K, Margolin AA, Kim S, et al. The Cancer Cell Line Encyclopedia enables predictive modelling of anticancer drug sensitivity. Nature. 2012;483:603–7. [PubMed: 22460905]
29. Luo B, Cheung HW, Subramanian A, Sharifnia T, Okamoto M, Yang X, et al. Highly parallel identification of essential genes in cancer cells. Proceedings of the National Academy of Sciences of the United States of America. 2008;105:20380–5. [PubMed: 19091943]
30. Kim J, Ji M, DiDonato JA, Rackley RR, Kuang M, Sadhukhan PC, et al. An hTERT-immortalized human urothelial cell line that responds to anti-proliferative factor. In vitro cellular & developmental biologyAnimal. 2011;47:2–9.
31. Rigby CC, Franks LM. A human tissue culture cell line from a transitional cell tumour of the urinary bladder: growth, chromosone pattern and ultrastructure. British journal of cancer. 1970;24:746–54. [PubMed: 5503601]
32. Marshall CJ, Franks LM, Carbonell AW. Markers of neoplastic transformation in epithelial cell lines derived from human carcinomas. Journal of the National Cancer Institute. 1977;58:1743–51. [PubMed: 864752]
33. Stegh AH, Schickling O, Ehret A, Scaffidi C, Peterhansel C, Hofmann TG, et al. DEDD, a novel death effector domain-containing protein, targeted to the nucleolus. The EMBO journal. 1998;17:5974–86. [PubMed: 9774341]
34. Arai S, Miyake K, Voit R, Nemoto S, Wakeland EK, Grummt I, et al. Death-effector domain-containing protein DEDD is an inhibitor of mitotic Cdk1/cyclin B1. Proceedings of the National Academy of Sciences of the United States of America. 2007;104:2289–94. [PubMed: 17283331]
35. Deng J, Carlson N, Takeyama K, Dal Cin P, Shipp M, Letai A. BH3 profiling identifies three distinct classes of apoptotic blocks to predict response to ABT-737 and conventional chemotherapeutic agents. Cancer Cell. 2007;12:171–85. [PubMed: 17692808]

36. Kim SH, Ricci MS, El-Deiry WS. Mcl-1: a gateway to TRAIL sensitization. Cancer research. 2008;68:2062–4. [PubMed: 18381408]

37. Wang L, Du F, Wang X. TNF-alpha induces two distinct caspase-8 activation pathways. Cell. 2008;133:693–703. [PubMed: 18485876]

38. Kurabe N, Mori M, Kurokawa J, Taniguchi K, Aoyama H, Atsuda K, et al. The death effector domain-containing DEDD forms a complex with Akt and Hsp90, and supports their stability. Biochemical and biophysical research communications. 2010;391:1708–13. [PubMed: 20043882]

39. Greig RG, Koestler TP, Trainer DL, Corwin SP, Miles L, Kline T, et al. Tumorigenic and metastatic properties of “normal” and ras-transfected NIH/3T3 cells. Proc Natl Acad Sci USA. 1985;82:3698–701. [PubMed: 3858844]

40. Bradley MO, Kraynak AR, Storer RD, Gibbs JB. Experimental metastasis in nude mice of NIH 3T3 cells containing various ras genes. Proc Natl Acad Sci USA. 1986;83:5277–81. [PubMed: 3523488]

41. Sharma P, Callahan MK, Bono P, Kim J, Spiliopoulou P, Calvo E, et al. Nivolumab monotherapy in recurrent metastatic urothelial carcinoma (CheckMate 032): a multicentre, open-label, two-stage, multi-arm, phase 1/2 trial. The LancetOncology. 2016;17:1590–8.

42. Ricci MS, Kim S-H, Ogi K, Plastaras JP, Ling J, Wang W, et al. Reduction of TRAIL-induced Mcl-1 and cIAP2 by c-Myc or sorafenib sensitizes resistant human cancer cells to TRAIL-induced death. Cancer Cell. 2007;12:66–80. [PubMed: 17613437]

43. Taniai M, Grambihler A, Higuchi H, Werneburg N, Bronk SF, Farrugia DJ, et al. Mcl-1 mediates tumor necrosis factor-related apoptosis-inducing ligand resistance in human cholangiocarcinoma cells. Cancer Res. 2004;64:3517–24. [PubMed: 15150106]

Implications

These studies identify MCL1 and DEDD as genes that contribute to aggressive urothelial carcinomas.

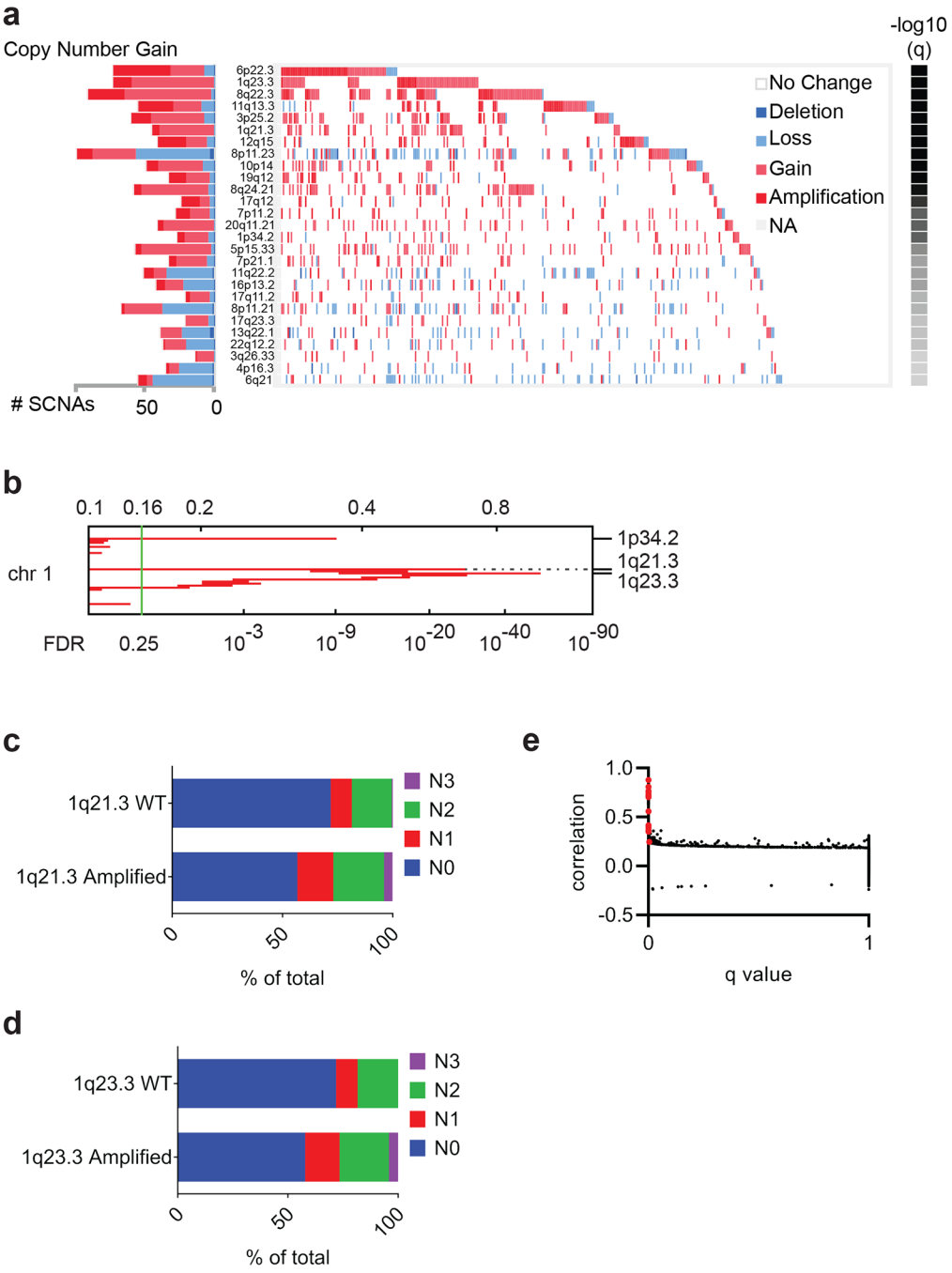

Figure 1: Copy number analysis of 408 UC patients from TCGA identifies 1q23.3 as a significant focal amplicon and identifies 1q21.3 as another significant amplicon on 1q.

a) 1q23.3 is the 2nd most significant amplicon in the TCGA Urothelial Carcinoma patient cohort. The left panel identifies the number of patients with the associated SCNA. The middle panel identifies each patient and the co-occurrences of any gains/amplifications (pink/red) or loss/deletions (light and dark blue). The right panel (which is how the figure is sorted) indicates the significance by q-value. 59 patients with gain (pink) of 1q23.3 and 14 patients with amplification (dark red). 1q21.3 is the 6th most significant amplicon with 39

patients with gain and 6 patients with amplification. Amplification is defined as log2(CN ratio) ≥ 1.3 while gain is a log2(CN ratio) > 0.58 and < 1.3.
b) Chromosome 1 GISTIC plots of UC patients from TCGA identifies two overlapping peaks in 1q21.3 and 1q23.3.
c) 43.3% of patients with 1q21.3 gain or amplification had nodal disease compared to 28.2% of patients without gain or amplification. p value = 0.00575 by Fisher's exact test.
d) 42.2% of patients with 1q23.3 gain or amplification had nodal disease (N1-N3) compared to 28.2% of patients without gain or amplification. p value = 0.00255 by Fisher's exact test.
e) Pearson correlation coefficients plotted against the associated q-value based on log2 measurements of genomic copy number and RNAseq expression of the corresponding gene. Red dots indicate genes identified in Table 2.

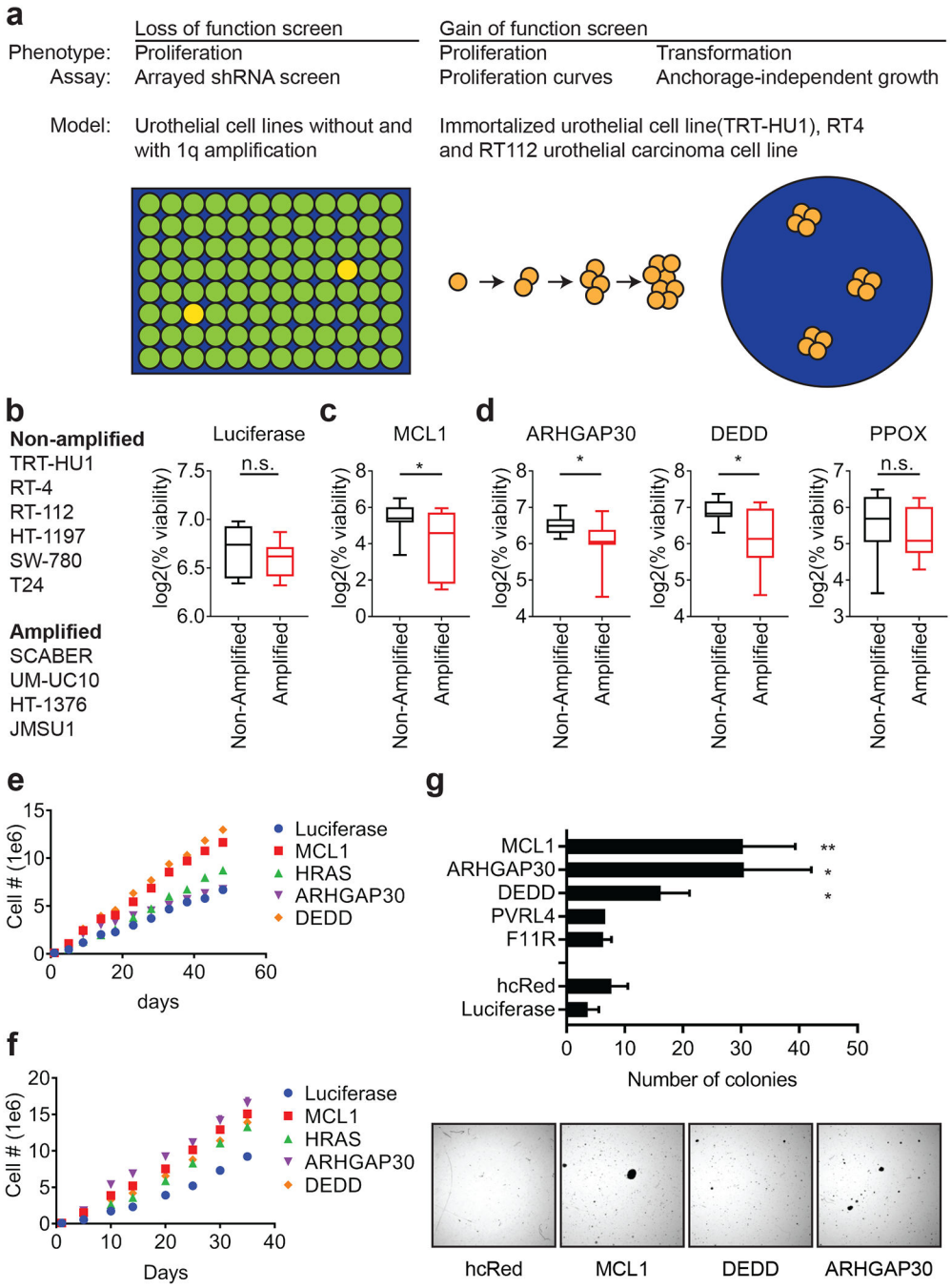

Figure 2: Two prong strategy utilizing both loss-of-function and over-expression studies to identify drivers of 1q in UC.

a) Schema of studies performed to identify functionally relevant genes in 1q21.3 or 1q23.3 amplified UC.

b) Amplified and Non-amplified cell lines used in this study. Average box plots of log2(% viability) between non-amplified lines as compared to amplified cell lines. Error bars reflective of standard deviation. Experiments were performed in biological replicates and in technical duplicates. Two-tailed p-value with n.s. as non-significant.

c) Box plot for an individual shRNA targeting *MCL1* between non-amplified and amplified cell lines. Error bars reflective of standard deviation. Experiments were performed in biological replicates. *Two-tailed p-value <0.05.

d) Box plot for individual shRNAs targeting ARHGAP30, DEDD and PPOX between non-amplified and amplified cell lines. Error bars reflective of standard deviation. Experiments were performed in biological replicates. *Two-tailed p-value <0.05.

e and f) Cell counts over time show MCL1 (red) and DEDD (orange) overexpression lead to a modest proliferative advantage in RT4 (e) and RT112 (f) cell lines when compared to control, Luciferase (blue). Experiments were performed in biological duplicate and representative data is shown from one replicate.

g) Soft agar assay in the RT112 cell line. Cells with overexpression of noted genes were plated in soft agar with a feeder layer and monitored for colony formation. Colonies were counted by ImageJ and representative images of colony formation shown below. Error bars reflective of standard deviation. Experiments were performed in biological triplicates and in technical triplicates. *Two-tailed p-value <0.05.

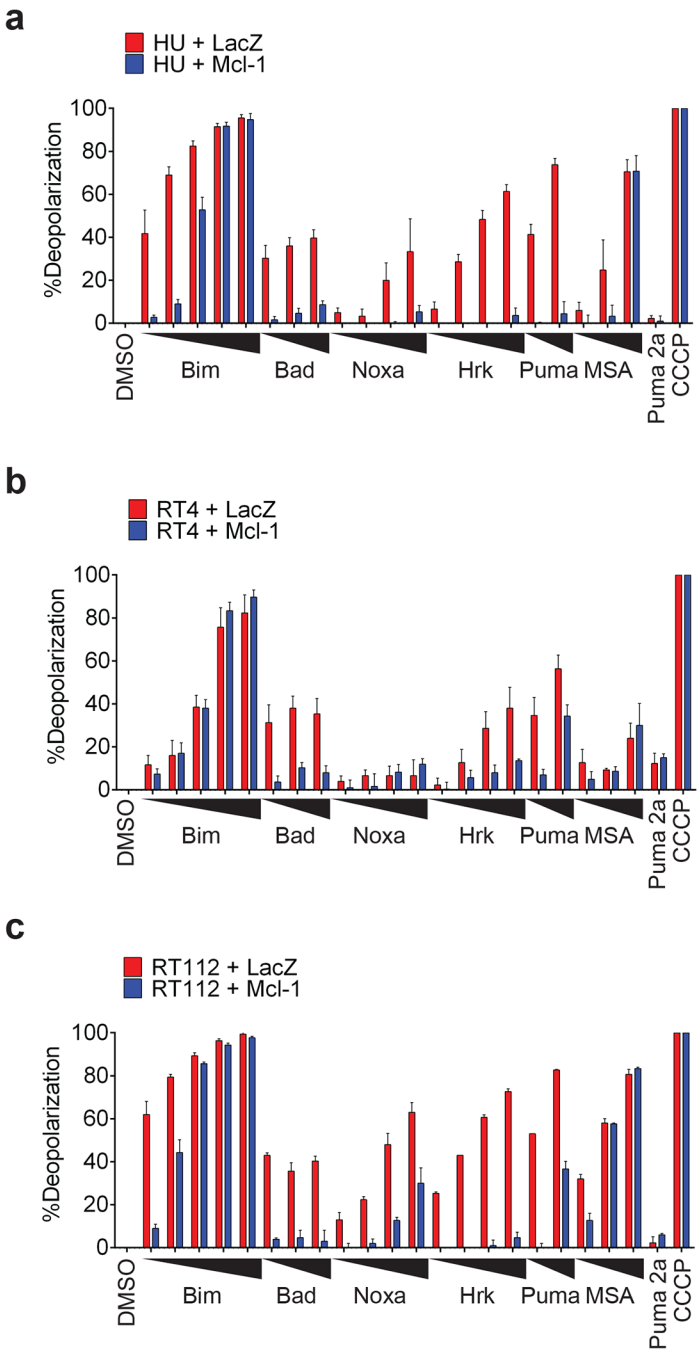

Figure 3: BH3 profiling of non-amplified urothelial cell lines with MCL1 overexpression consistent with an MCL1 dependent intrinsic apoptotic signature. DMSO serves as the negative control as exposure of cells to DMSO led to no evidence of depolarization or MOMP activation. Carbonyl cyanide m-chlorophenyl hydrazine (CCCP) inhibits oxidative phosphorylation and is a positive control.

a-c) Treatment of the noted cell line with either LacZ or MCL1 overexpressed with DMSO or a BH3 mimetic. Increased depolarization is indicative of increased apoptotic potential. No increased depolarization with low concentrations of BIM, with NOXA or with HRK. Experiments were performed in biological triplicate and error bars are standard deviations.

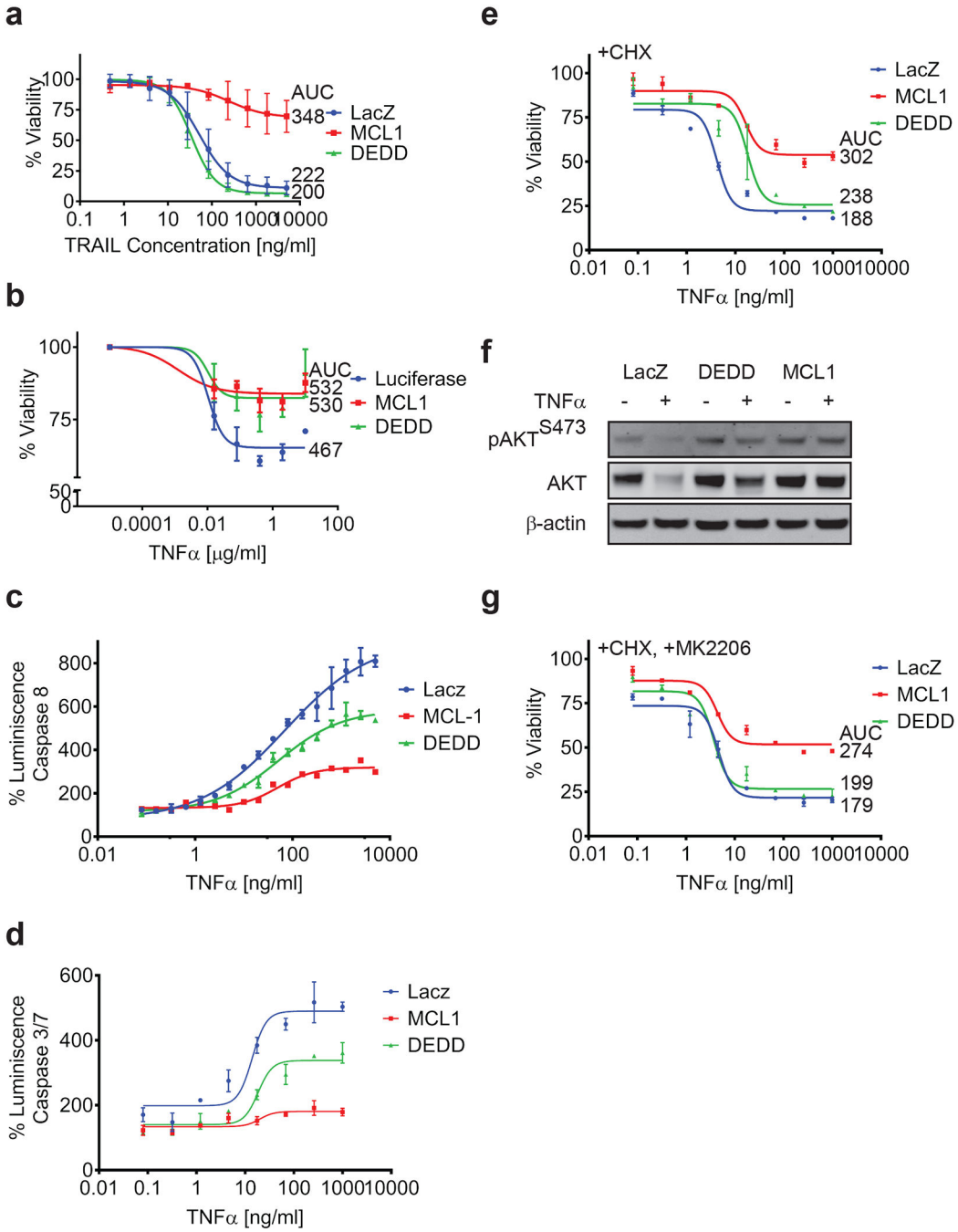

Figure 4: MCL1 is a pan anti-apoptotic protein while DEDD is a TNFα anti-apoptotic protein in RT112.

a) MCL1 but not DEDD resists TRAIL induced apoptosis as measured by CellTiter-Glo. Error bars are standard errors of the mean and representative of 3 technical replicates. AUCs (% viability * ng/mL) listed on the right. Experiments representative of two biological replicates.

b) MCL1 and DEDD resists TNFα induced apoptosis as measured by CellTiter-Glo. Cells were treated with increasing doses with TNFα and viability was measured by CellTiter-Glo

after 6 hours. AUCs (% viability * μg/mL) listed on the right. Error bars are standard deviations and representative of 2 biological replicates.

c) MCL1 and DEDD resists TNFα induced apoptosis but to different degrees as measured by activation of Caspase 8 activity. Error bars are standard errors of the mean and representative of 3 technical replicates.

d) MCL1 and DEDD resists TNFα induced apoptosis but to different degrees as measured by activation of Caspase 3/7 activity. Error bars are standard errors of the mean and representative of 3 technical replicates. Experiments representative of two biological replicates.

e) Addition of cycloheximide sensitizes DEDD to TNFα at high concentrations. Addition of 1uM of cycloheximide with increasing concentrations of TNFα for 6 hours leads to resistance to TNFα induced apoptosis in both MCL1 and DEDD. At 100ng/mL DEDD overexpressed cells were similarly sensitive as LacZ controls. AUCs (% viability * ng/mL) listed on the right.

f) Akt and pAkt (S473) is increased upon TNFα treatment in MCL1 and DEDD. Immunoblots of RT112 cells with or without treatment with TNFα. Immunoblots representative of 3 biological replicates.

g) Addition of MK2206 abrogates DEDD's and partially MCL1's ability to resist TNFα induced apoptosis as measured by CellTiter-Glo. AUCs (% viability * ng/mL) listed on the right. Error bars are standard errors of the mean and representative of 3 technical replicates. Experiments representative of two biological replicates.

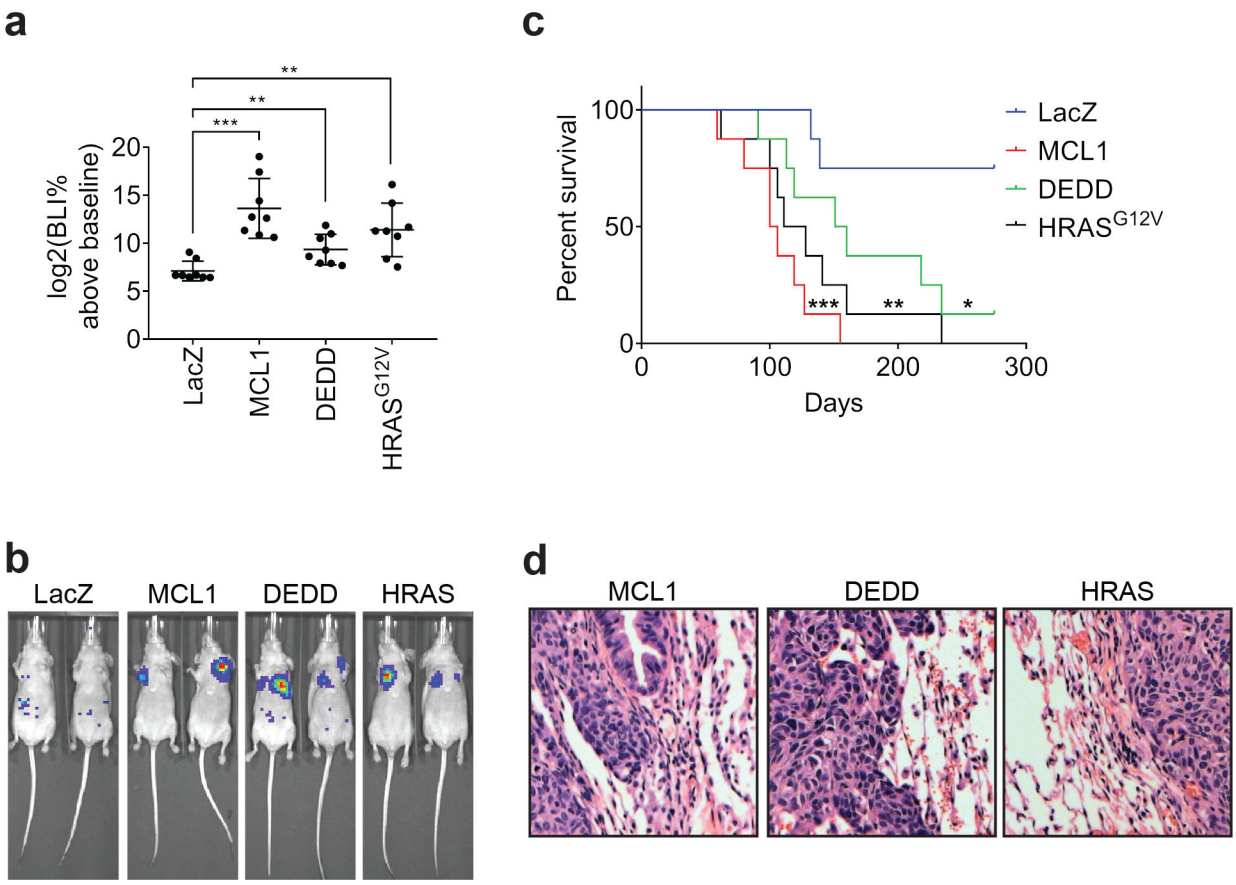

Figure 5: DEDD and MCL1 overexpression lead to experimental metastasis in vivo.

a) NCr-Nude mice from Taconic Laboratories were injected with cells overexpressing LacZ, MCL1, DEDD or HRAS^{G12V} in RT112 cells (8 per cohort). At 56 days, mice were injected with luciferase and bioluminescence imaging (BLI) was performed. Compared to LacZ, MCL1, DEDD and HRAS^{G12V} had significantly higher BLI. **p<0.005 and ***p<0.0005

b) Representative images of mice

c) Kaplan Meyer curves of mice with tail vein injections (8 mice per cohort). Overexpression of DEDD, MCL1 and HRAS^{G12V} led to significant mortality (e.g. respiratory distress) over the course of 275 days. *p<0.05, *p<0.005, *p<0.0005 based on Mantel-Cox tests.

d) Representative images of histology from pulmonary metastasis

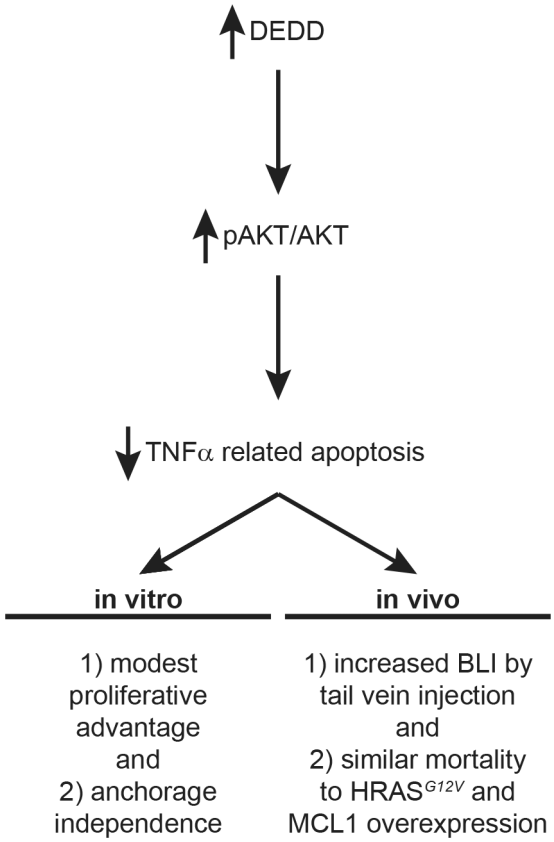

Figure 6:
Summary of effects on urothelial carcinoma cell lines from DEDD overexpression.

Table 1:

Genes identified as focally amplified in 1q21.3.

1q21.3
ADAMTSL4
ARNT
C1orf138
CTSK
CTSS
ENSA
GOLPH3L
MCL1
HORMAD1
MIR4257
SNORA40
RN7SL600P
RN7SL473P

Table 2:

Genes identified as focally amplified in 1q23.3.

Chr1 location (UCSC hg19)	Riester et al	From TCGA	In this study
160,965,001	F11R	F11R	F11R
161,007,422		TSTD1	TSTD1
161,009,041		USF1	USF1
161,016,732		ARHGAP30	ARHGAP30
161,040,781		PVRL4	PVRL4
161,068,181		KLHDC9	KLHDC9
161,070,346	PFDN2	PFDN2	PFDN2
161,087,862			NIT
161,090,769	DEDD		DEDD
161,123,534			UFC1
161,129,254	USP21		USP21
161,136,181	PPOX		PPOX